Article

Not peer-reviewed version

Ignition delay and burning rate analysis of diesel-carbon nanotube blends stabilized by surfactant: a droplet scale study.

Anderson Gallego *, Karen Cacua, David Gamboa, Jorge Luis Rentería Peláez, Bernardo Herrera

Posted Date: 18 October 2023

doi: 10.20944/preprints202310.1042.v1

Keywords: Ignition delay; Burning rate; Carbon nanotubes; Commercial diesel; sodium dodecylbenzene sulfonate.

Article

Ignition Delay and Burning Rate Analysis of Diesel-Carbon Nanotube Blends Stabilized by Surfactant: A Droplet Scale Study

Anderson Gallego [1,2,*], Karen Cacua [1], David Gamboa [1], Jorge Rentería [1] and Bernardo Herrera [1]

[1] Advanced Materials and Energy Group (MATyER), Instituto Tecnológico Metropolitano, Street 54A No 30 – 01, Medellín, Colombia.

[2] Group of Research and Innovation in Energy (GIIEN), Institución Universitaria Pascual Bravo, Street 73 No 73a – 226, Medellín, Colombia.

* Correspondence: anderson.gallego@pascualbravo.edu.co

Abstract: In this study, ignition delay and burning rate are experimentally investigated in relation to the effect of pristine carbon nanotubes (CNTs), sodium dodecylbenzene sulfonate (SDBS), and diesel blends. Single droplet combustion tests were conducted in a combustion system for 21 days using CNTs at concentrations of 50 ppm and 100 ppm, that were dispersed in Colombian commercial diesel and stabilized by SDBS. Additionally, recordings of the combustion were collected, and the Shadowgraph optical method was utilized for monitoring the evolution of droplet size during combustion. The measurements were done over a four-week period. The results demonstrated that the temporal stability has a direct impact on the single droplet combustion tests because a concentration of CNTs of 100 ppm showed higher stability than those achieved by 50 ppm. Consequently, improvements were found with a concentration of 100 ppm, for instance, thermal conductivity increased by about 20%, ignition delay time by 16.2%, and burning rate by 30.5%.

Keywords: ignition delay; burning rate; carbon nanotubes; commercial diesel; sodium dodecylbenzene sulfonate

1. Introduction

Compression ignition engines (MEC) are a technology that uses the diesel cycle as its basic operating principle, admitting air first and then injecting high-pressure diesel when the piston is close to the top dead center. The temperature and pressure conditions generate combustion, which encourages the piston to generate work. They have a significant impact on several oil-based economic sectors, including transportation, electricity production, and agricultural machines, among others. Compared to other technologies like gasoline engines, they are more durable, more cost-effective, and have higher thermal efficiency [1]. However, a problem with this technology is the release of pollutants and their impact on the environment and public health. As a result, there are government laws, such those provided by the EURO 6 standard, which have stablished minimum pollutant gases emissions from automotive industry [2]. Although the EURO regulation was introduced in 1992, work is still being done on the EURO 7 to take drastic action and control the operations of internal combustion engines [3]. In fact, it is predicted that production of fossil fuel-based engines would cease in the near future due to efforts to move to a fossil fuel-free economy and energy transition [4].

However, internal combustion engines have advantages over other technologies such as electric and hybrid automotive. Therefore, a number of alternatives are being offered with the goal of preserving the technology of actual engines. Research has concentrated on several alternatives, including the use of biodiesel [5,6], the utilization of natural gas for dual-mode operation [7], and the usage of nanofuels by dispersing nanomaterials in diesel, biodiesel, or a combination of both [8,9]. The use of nanofuels is one of the methods that try to lessen the environmental impact of internal combustion engines, especially compression ignition engines. These materials provide high energy density, low sulfur content and high volatility [10,11]. Additionally, they serve as thermal bridges

 doi:10.20944/preprints202310.1042.v1

inside the fuel during combustion, speeding up the chemical reaction and improving parameters such as the ignition delay, combustion rate, and the oxidation of pollutants like unburned hydrocarbons (HC) and carbon monoxide (CO) [12].

However, there have been increasing concerns regarding the use of metallic and metallic oxide nanomaterials, such as titanium dioxide (TiO_2) [6], cerium oxide (CeO_2) [13], copper (Cu) and copper oxide (CuO) [14], among others. This is because these nanomaterials have negative effects on human health due to their high chemical reactivity and biological activity. They can generate genotoxicity and biochemical toxicity as they can easily penetrate the skin or enter the body through inhalation or ingestion of water or food [15]. Therefore, some researchers have justified the use of carbonaceous nanomaterials. For example, Heidari-Maleni, et al. [16] highlighted the biocompatibility and non-toxicity of graphene quantum dot (GQDs), which also helped to reduce the duration of combustion and improved the rate of heat release when used in a diesel engine.

Moreover, Alenezi et al. [16] used mixtures of diesel and biodiesel with multi-walled carbon nanotubes (MWCNTs). They discovered that their application in a diesel engine resulted in better atomization of the fuel and, as a result, higher pressures inside the cylinder, which was 4.67% higher than the maximum pressure reached with operation in diesel mode. Bello, et al. [17] also used nanomaterials made of GO, TiO_2, and GO doped with TiO2 (GO-TiO2). They found decreased emissions of particulate matter (PM) and an increase in the thermal performance of the engine by up to 8.36%, which was owing to the fuel's higher reactivity and improved combustion caused by the presence of nanomaterials.

Furthermore, diesel, biodiesel, and their blends are well known to be injected as atomized droplets. The phenomena that these fuel droplets undergo inside the combustion chamber are probably what determine the emissions and performance of a diesel engine. Therefore, the study of individual droplet combustion characteristics can explain phenomena such as those obtained with the presence of nanomaterials because they may benefit combustion due to increases in thermal conductivity, radiation absorption [18], the formation of layers of nanoparticles that improve heat conduction to the interior of the droplet, and microexplosions [19]. Consequently, a phenomenological approach to droplet combustion can be applied to approximate the impact of nanomaterials on the performance and emissions of a compression ignition engine.

For instance, Ooi, et al. [20] demonstrated improvements in fuel drop combustion characteristics such as ignition delay, combustion temperature, and combustion duration when graphite oxide (GO), aluminum oxide (Al_2O_3), and cerium oxide (CeO_2) were used. As a result, improved thermal efficiency and lower emissions of pollutants like NO_X, PM, and CO were predicted when those nanomaterials were used in a diesel engine. Additionally, Ooi et al. [21] found similar results in another of their works using GO nanomaterials dispersed in diesel and biodiesel. They claimed that GO can aid in reducing the ignition delay and increasing the burning rate due to the properties already mentioned and additionally, oxygen-supplying capacity, and exothermic reactions. Also, Abdul Rasid and Zhang [22] underlined the existence of a nanoparticle shell on the droplet surface during the evaporation process when dispersed soot nanoparticles in the fuel, which favors heat transfer towards the core of the droplet. Likewise, Singh et al. [23] confirmed that using multi-walled carbon nanotubes (MWCNTs), the evaporation rate can be accelerated due to the radiation absorption.

Despite the advantages, nanomaterial aggregation and sedimentation have a detrimental impact on the expected benefits of nanomaterials dispersed in liquid fuels, which are the main concerns with their usage [24]. Accordingly, some studies have employed the functionalization [25] and surfactant [26] approaches. For instance, surfactant addition has been shown to increase the stability of the dispersions while maintaining the features of the nanomaterials dispersed in diesel without altering the fuel's characteristics [27,28]. Furthermore, when nanofuels are used in diesel engines, adding surfactant reduced nanoparticle deposition on injectors, valves, and fuel lines [29].

According to Wang, et al. [30], the evaporation of single droplets of diesel and biodiesel is comparable when surfactants (span80 and tween80) are used with those fuels. As a result, using nanomaterials of CNTs and surfactant may improve droplet evaporation rate in those fuels. Likewise,

 doi:10.20944/preprints202310.1042.v1

Kannaiyan et al. [31] noted that the use of Span80 had no impact on the experiment's outcomes, which were exclusively related to the usage of Al_2O_3 nanoparticles and their stability, which is due to the fact that surfactant molecules attach to the nanoparticle surfaces and create an absorption layer around them. Consequently, nanoparticle collisions undergo electrostatic repulsive forces that overcome Van der Waals attraction [32]. Thermal conductivity, viscosity, and surface tension, for example, remain unchanged at lower surfactant concentrations [33,34]. Nonetheless, Liang et al., [35] found that using a blend of bioethanol and oleic acid as a surfactant improves combustion parameters such as ignition delay, burning rate, and temperature are improved with respect to only bioethanol. Nevertheless, surfactants have only been utilized in experimental research to keep nanofuels chemically stable [36], and their effects on single droplet combustion and temporal stability, as well as those carbonaceous nanomaterials like CNTs dispersed in diesel fuel, have not been thoroughly studied in the literature.

Therefore, this study performs for the first time an experimental analysis of combustion parameters like ignition delay and burning rate of a single droplet from a dispersion of pristine carbon nanotubes in commercial diesel from Colombia that has been stabilized with sodium dodecyl benzene sulfonate (SDBS). These results are related to stability analysis across a three-week period as determined by measurements of dynamic light scattering (DLS), pH, potential Zeta, among others, and properties such as thermal conductivity and surface tension. In terms of combustion efficiency and pollutant emissions, the characterization of the ignition delay and burning rate of these blends offer helpful information about how they would function in actual ignition compression engines.

2. Methodology

2.1. Nanofuels preparation and characterization

Commercial pristine carbon nanotubes (CNTs) from the company SkySpring Nanomaterials, Inc. were used for the preparation of the nano-fuels. The technical specifications of the CNTs are found in Table 1. Additionally, a scanning electron microscopy (FE-SEM) in a JEOL JSM7100F (JEOL Ltd., Japan) was also used to confirm the morphology and size of the CNT nanoparticles (Figure 1). In the first phase, nanomaterials were dispersed in Colombian commercial diesel (B10, 90% diesel, and 10% palm oil biodiesel) in a vessel with 50 mL of nanofuel. The nano-fuels were prepared using the two-step method [14] and, two concentrations of CNTs were used: 50 ppm and 100 ppm. To maintain the stability of the dispersion, the anionic surfactant sodium dodecylbenzene sulfonate (SDBS, Sigma–Aldrich Pty. Ltd.) was used as a dispersing agent at a concentration of 0.02 w/v%. A Precisa EP225-DR microbalance (Precisa, Switzerland) was used to weigh the nanomaterials and the surfactant. SDBS and diesel blends were homogenized through a Branson 1800 ultrasonic bath before CNTs were added. A UP400St sonicator (24 kHz, Hielscher, USA) served to break agglomerates and disperse the nanomaterials in the diesel. During this procedure, the ultrasound equipment was set to 50% amplitude for 1 hour. The main steps of this method are outlined in Figure 2, and the physicochemical properties of the base fuel and the resultant nanofuels are shown in Table 2.

Preprints (www.preprints.org) | NOT PEER-REVIEWED | Posted: 18 October 2023 doi:10.20944/preprints202310.1042.v1

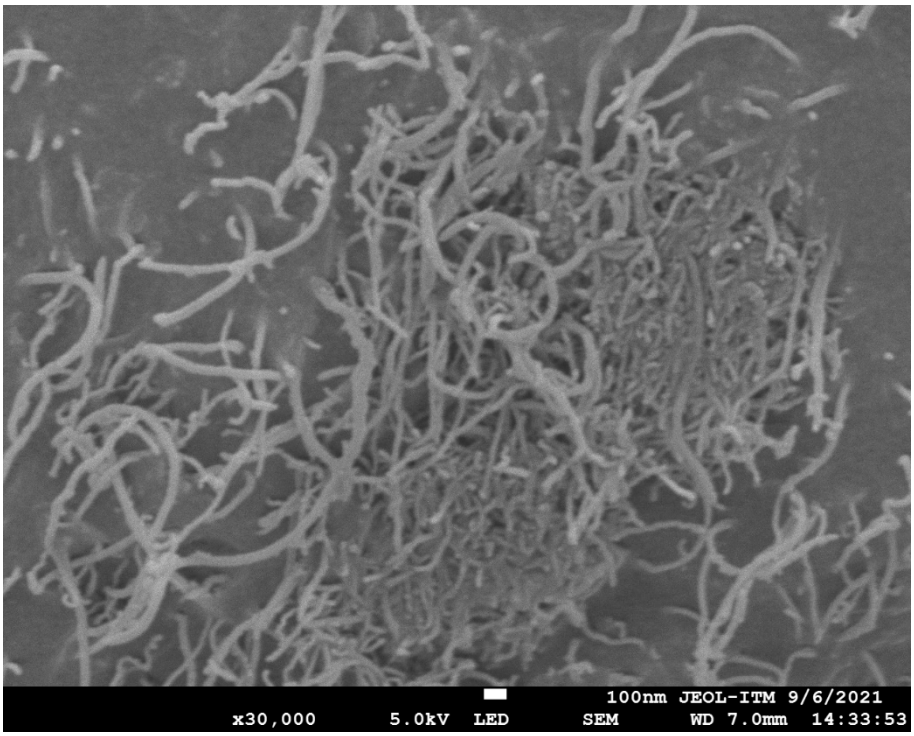

Figure 1. SEM images of CNT nanoparticles.

Table 1. Technical specifications of the carbon nanotubes used in this study.

Type	Specification
Purity	>95 %
External diameter	20-30 nm
Internal diameter	5-10 nm
Length	10-30 μm
Surface area	>110 m^2/g
Density	2.1 g/cm^3

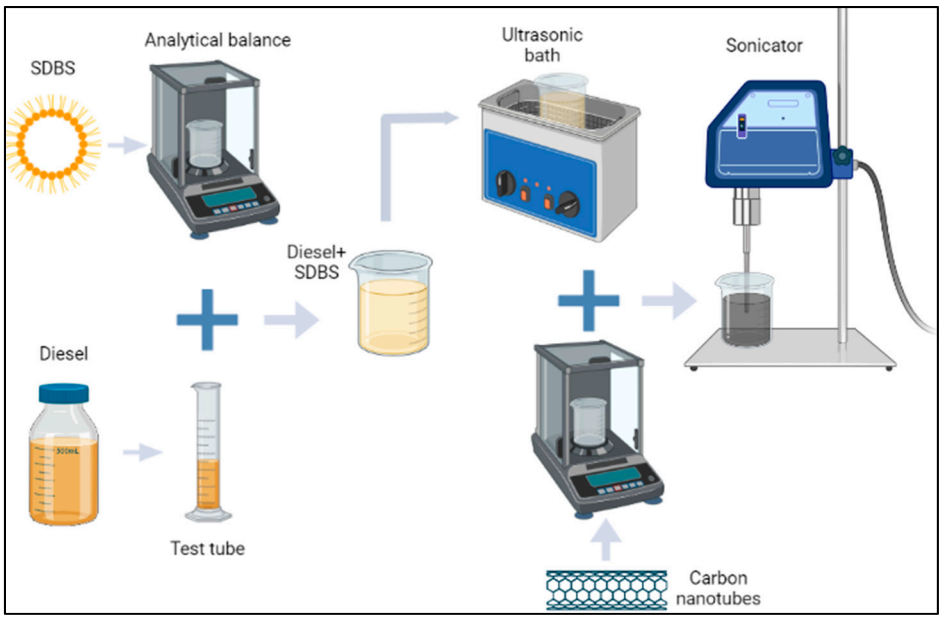

Figure 2. Nanofuels preparation method. Created with Biorender.com.

Preprints (www.preprints.org) | NOT PEER-REVIEWED | Posted: 18 October 2023 doi:10.20944/preprints202310.1042.v1

On the other hand, after the nanofuels were made, they were tested to see how stable they were. The first parameter measured was the Zeta potential, which is the net surface charge of the nanomaterials in suspension. This measurement was carried out on a Nanoplus Particle Analyzer (Micromeritics Instrument Corporation, USA) after each time the nanofuels were made. Likewise, a dynamic light scattering (DLS) analysis was performed over the course of 21 days, with measurements being taken every seven days. This was done to identify variations in the sizing of the nanomaterials in suspension. At the same time, photographs were taken to visually detect the sedimentation of the nanofuels at the moment of preparation and during the same days that the DLS measurements were made.

Table 2. Physicochemical properties of the fuels and nanofuels.

Property	Unit	Diesel	Diesel + SDBS	Diesel + SDBS + CNT 100 ppm	Standard
Kinematic viscosity at 40 ◦C	mm²/s	3.771	4.374	4.469	ASTM D445
Cetane index	-	48.68	48.90	48.80	ASTM D976
Heating value	MJ/kg	45.14	44.94	44.92	ASTM D240
API gravity of petroleum products at 15.6 °C	°API	33.2	31.8	31.8	ASTM D287
Gum content in fuel by evaporation jet	mg/100 ml	49.5	35.5	15.5	ASTM D381
Pour point	°C	-15	-12	-12	ASTM D97
Flashpoint	°C	71	72	73	ASTM D93
Cloud point	°C	2	-1	-6	ASTM D2500

Additionally, thermal conductivity measurements were performed using a KD2 Pro Thermal Properties Analyzer (Decagon Devices, Inc., Pullman, WA, USA). This device uses the transient hot-wire approach as the basis for its operation. Such property was obtained at two temperatures, 20 °C and 60 °C, which were adjusted using a thermostatic bath. For each nanofuel, about ten experiments were performed right away after their preparation, ensuring that at least 15 minutes were given between measurements to allow for temperature stability. Under the identical conditions, the surface tension of the blends was measured using the Du Noüy ring method, utilizing a surface tensiometer Attention Sigma 701 (Biolin Scientific) and a thermostatic bath for temperature control. Furthermore, an ORION A325 pH/conductivity potable meter (Thermo Scientific™, USA) was used to measure the pH change of nanofuels in relation to commercial diesel. Once the nanofluids were prepared, measurements were made at room temperature. Finally, the thermal behavior of nanofuels samples was characterized using a thermogravimetric analyzer (Discovery 550 – TA Instruments). A 50 mg sample was heated in a nitrogen atmosphere between 25 and 250 °C at a rate of 10 °C/min. Thermogravimetric analysis was done under these conditions to examine the influence of carbon nanotubes on fuel evaporation rates, which have a substantial impact on reactant mixing inside the cylinder. This affects the ignition delay and fuel burning rates [37,38]. Furthermore, this test is commonly conducted to verify that the additive under consideration lacks a negative impact on fuel boiling points, which can be problematic in internal combustion engines [39,40]

2.2. Experimental procedure

Evaluation of fuel properties, including ignition delay and combustion rate, was done to determine the impact of adding carbonaceous nanoparticles to the fuel and their temporal stability. This was done by following the methodology presented by Ooi et al. [12], Mosadegh et al. [41] and Wang et al. [42]. Figure 3 shows a schematic representation and experimental setup of droplet

Preprints (www.preprints.org) | NOT PEER-REVIEWED | Posted: 18 October 2023 doi:10.20944/preprints202310.1042.v1

combustion. A Chronos 1.4 high speed camera (1) was used to obtain the images of the combustion of the diesel droplet (6), this camera has an image sensor of 8.45 x 6.76mm with a Fill rate of 1.4 Gpx/s, which allows you to record up to 38565 FPS at a resolution of 336 x 96. In this case, because high-quality images are needed for post-processing, the recording configuration used was 1057 FPS at a resolution of 1280 x 1024.

Furthermore, a data acquisition system (2) was used to process the temperature information obtained by the thermocouple (4), as well as to control the recording of the camera. Two biconvex lenses (3) were used to collimate the light rays towards the sample and the camera lens. With this configuration, a uniform background was obtained for the camera, and the light refracted (8) by the droplet allowed images to be taken with a defined the droplet outline. therefore, the shadowgraph optical technique was used to follow the droplet size evolution during the combustion process [43,44].

Each experimental test begins with the aggregation a droplet of 3 µL of fuel through a micropipette in the middle of two crossed silicon carbide wires. Then two pneumatic cylinders (7) on the sides each move an electrical resistance (5) that serves as ignition system of fuel droplet. A control system run by an Arduino processor was used to finally synchronize the system with the heating of the electrical resistances and the activation of the pneumatic cylinders.

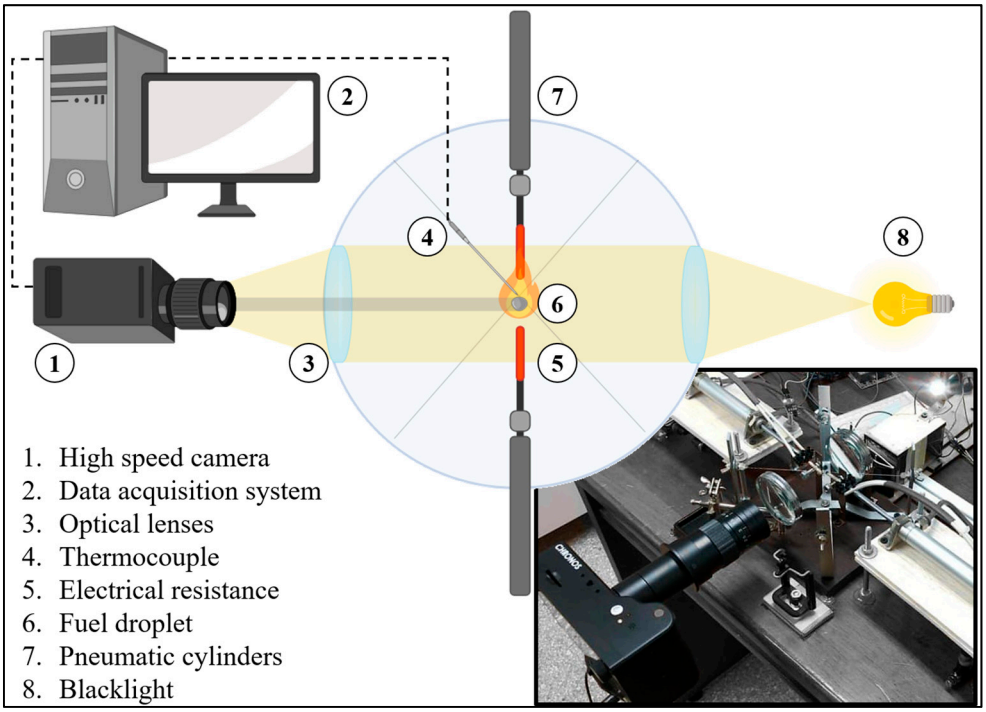

Figure 3. Schematic representation and experimental setup of droplet combustion.

In addition, the results are shown for the normalized area of the drop (A/A_0), whose purpose is to show the relationship between the area of the drop at a given moment in time with respect to the initial area. Thus, the work proposed by Law [45] was followed, who proposes models for transitory heating and combustion processes of fuel droplets, where the phenomenon of ignition and extinction is explained through kinetic models. The model starts from the explanation of the propagation speed of the fuel flame, which can be calculated from the combustion rate constant (K) and following the D^2 law as shown in equation (1).

$$D^2 = D_0^2 - Kt \tag{1}$$

The ignition delay was obtained at 95% of the time at which the maximum expansion area occurs [41]. The droplet normalized area variation analysis with respect to time was carried out using the methodology developed in a previous work using a Matlab code [43]. The algorithm is divided into three stages. In the first stage the extraction of each video frame of droplet combustion process is

Preprints (www.preprints.org) | NOT PEER-REVIEWED | Posted: 18 October 2023 doi:10.20944/preprints202310.1042.v1

made, in the second stage for each frame a cut on the region where the combustion process occurs is made, finally in the third stage the image is binarize to obtain the droplet normalized area variation with respect to time.

2.3. Data reduction

Table 3 shows the uncertainty of the equipment used to perform the analyses TGA, SEM, DLS, and weigh measurement. In the case of the TGA, the maximum relative uncertainty in the measurement of temperature is 4%, which occurs at the beginning of the analysis, and this relative uncertainty reduces up to 0.4% at the highest temperatures. Moreover, the uncertainty of mass balance introduces a maximum relative uncertainty of 0.002% in the nanofuels concentration, while the maximum relative uncertainty of the hydrodynamic diameter measured with DLS is 0.02%. The uncertainty of the SEM does not introduce uncertainty in the results because we did not measure any variable with this instrument, which was used only for a qualitative characterization of the carbon nanotubes morphology.

Furthermore, as in our previous work [43], the droplet area was determined by counting the pixels in the binarized image. Therefore, our uncertainty analysis is limited to the standard deviation of the tests. Thus, three replicates of each fuel preparation were developed and burnt every week as indicated above, with each set of tests consisting of burning ten droplets and, thereby, the normalized area (A/A_0) curve was obtained. The ignition delay and burning rate were then calculated.

Table 3. Uncertainty of the instruments used in the characterization and preparation of the nanofuels.

Parameter	Instrument	Uncertainty
Thermogravimetric analysis	TA Instrument SDTQ 600	$\pm 1 \times 10^{-7}$ g and ± 1 °C
Scanning Electron Microscopy	JEOL JSM-7100F	± 1.2 nm
Dynamic Light Scattering (DLS)	Micromeritics Nanoplus HD	± 0.1 nm
Carbon nanotubes weight	Precisa EP225-DR	$\pm 1 \times 10^{-6}$ g

Results shows that each time step has a distinct standard deviation, therefore, the minimum, maximum, and average coefficients of variation of the A/A_0 ratio for each fuel and nanofuel are calculated and displayed in Table 4. Such coefficients express the standard deviation as a percentage of the arithmetic mean, providing a relative interpretation of the degree of variation in the results between each replicate. The highest values achieved, as shown in Table 4, are close to 23.24%. Thus, the A/A_0 mean value may be regarded as representative of the data set and the measured data for the A/A_0 ratio at each time step is considered to be homogenous (less than 30%).

Table 4. Maximum, minimum, and average coefficients of variation for each fuel and nanofuel during the course of the test.

Fuel/nanofuel	Day of the tests	Coefficient of variation of A/A_0		
		Maximum	Minimum	Mean
Diesel	-	19.63%	0.04%	2.11%
Diesel + SDBS	-	12.70%	0.01%	1.56%
Diesel + SDBS + CNT 50 ppm	Preparation day	20.40%	0.02%	2.49%
	7 days	18.64%	0.01%	2.21%
	14 days	18.76%	0.01%	1.93%
	21 days	15.46%	0.01%	1.86%
Diesel + SDBS + CNT 100 ppm	Preparation day	19.52%	0.02%	2.86%
	7 days	14.86%	0.02%	1.89%
	14 days	23.24%	0.02%	3.50%
	21 days	12.92%	0.02%	1.96%

Preprints (www.preprints.org) | NOT PEER-REVIEWED | Posted: 18 October 2023 doi:10.20944/preprints202310.1042.v1

The ignition delay and burning rate uncertainty was calculated using a similar method. However, they lack the uncertainty associated with measurement equipment, therefore for ignition delay, the period in which the A/A0 ratio is 95% of the highest value of the ratio was chosen as the delay time for this work. As a result, the ignition delay uncertainty was taken as the coefficient of variation for each experimental condition, taking into consideration the replicates included in the standard deviation. Likewise, burning rate was calculated through the D^2 law which also depends on the A/A_0 ratio. Table 5 shows the coefficient of variation (the ratio between the standard deviation and the mean) of ignition delay and burning rate for each fuel and nanofuels, which are considerably lower than 30%, indicating that the data set is homogeneous.

Table 5. Coefficients of variation of the ignition delay and burning rate for every fuel and nanofuels during the test.

Fuel/nanofuel	Day of the tests	Coefficient of variation of the ignition delay	Coefficient of variation of the Burning rate
Diesel	-	1.76%	5.98%
Diesel + SDBS	-	2.17%	3.16%
Diesel + SDBS + CNT 50 ppm	Preparation day	1.87%	4.03%
	7 days	3.89%	2.92%
	14 days	1.12%	7.00%
	21 days	2.13%	8.18%
Diesel + SDBS + CNT 100 ppm	Preparation day	3.22%	5.16%
	7 days	2.41%	2.80%
	14 days	2.59%	4.33%
	21 days	3.30%	4.92%

3. Results and discussion

In order to estimate the ignition delay and combustion rate, the experimental results are explained in the following subsections. In addition, a brief explanation of the results supported by a nanofuels temporal stability analysis is given.

3.1. Stability analysis

Figure 4a shows a quantitative description of the stability, which is given by the dynamic light scattering (DLS) measurements. This method analyzes the Brownian motion by detecting the oscillations of the light scattered by nanoparticles moving in the fuel at different speeds. Thus, the DLS relates the nanoparticles average speed to their size. In this case, the size increased during 21 days from 540 and 509 nm up to 1317 and 913 nm for CNTs at 50 ppm and 100 ppm, respectively. The size increments are the main consequence of the agglomeration and sedimentation of nanomaterials, which, in turn, occur due to the high surface energy of the nanoparticles, the van der Waals forces, and the collisions between nanoparticles caused by the Brownian motion.

According to the literature, the higher the concentration of nanomaterials, the larger the hydrodynamic size tested using DLS [46]. In this case, however, the addition of the surfactant SDBS produced the opposite effect since the hydrodynamic sizes were lower at 100 ppm than at 50 ppm. This effect can be related to under typical surfactant dispersions in diesel, molecules tend to form micelles, which are groupings of molecules that form generally spherical forms when their polar ends interact. However, in certain conditions, particularly when using low quantities of nanomaterials, surfactants probably will form macromolecules (micelles or high quantities of a group of molecules), which led to a depletion in the stabilization [47].

Therefore, when a CNT concentration of 50 ppm was dispersed with a concentration of SDBS of 0.02 w/v%, the surfactant concentration proves to be too high and probably macromolecules were formed. In contrast, a concentration of CNTs of 100 ppm results in a high probability of interactions between SDBS and CNTs because SDBS attaches to the surface of CNTs and creates an absorption

Preprints (www.preprints.org) | NOT PEER-REVIEWED | Posted: 18 October 2023 doi:10.20944/preprints202310.1042.v1

layer that surrounds the nanomaterials and prevents the creation of macromolecules [48]. Therefore, in the presence of SDBS, a concentration of 50 ppm exhibits worse stability than that of 100 ppm.

The above is validated with the visual inspection shown in Figure 4b, where the nanofuels tested are displayed. A CNT concentration of 100 ppm exhibits dispersed nanoparticles over the course of the visual inspection. Meanwhile, CNTs concentration of 50 ppm shows sedimentation after fourteen days, as indicated by the blue line. Additionally, a noticeable distinction between the liquid and solid phases can also be seen. This results in a clearer black color due to changes in the colloidal suspension, which are related to the low stability of the concentration.

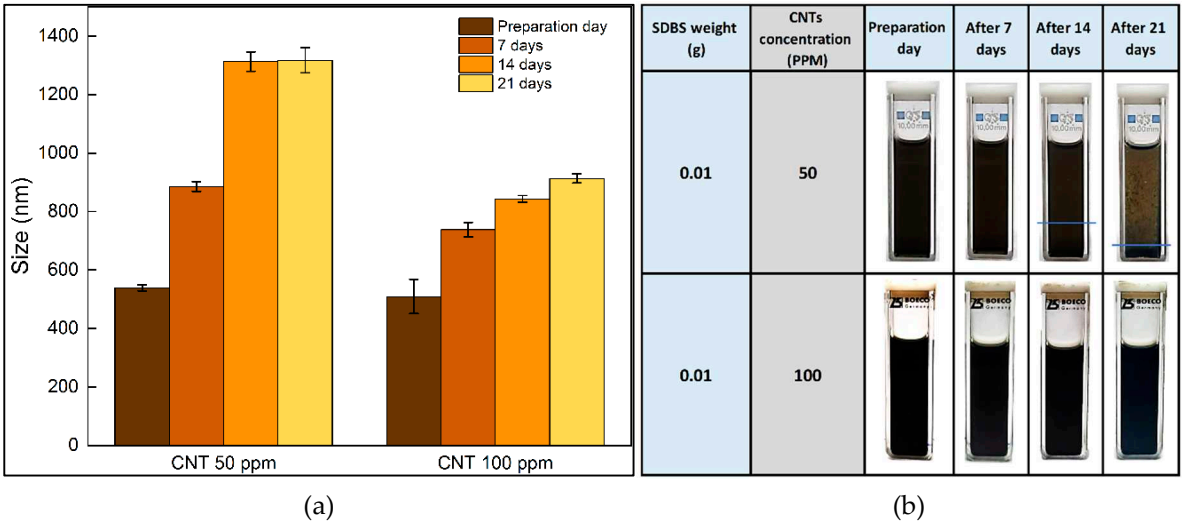

(a) (b)

Figure 4. Characterization of the hydrodynamic size of CNTs in the nanofuels (a) DLS results and (b) visual inspection for different days after nanofuels preparation. The size increases because CNT nanomaterials were agglomerating inside the fuel over the days, which causes sedimentation.

Figure 5 shows the changes in pH and zeta potential caused by the addition of SDBS to CNT concentrations of 50 ppm and 100 ppm. The graphs are displayed together because the pH values affect the zeta potential, which alters the electrical charge density on the surface of the nanoparticles and can cause repulsive forces between nanoparticles that are dispersed [49]. The result shows that the pH related to diesel without nanoparticles and SDBS was near 4.8. Thus, with the SBDS addition, pH was raised to 5.4 and the zeta potential was -28.3 mV. These values are due to the anionic nature of SDBS, and, therefore, the surface charge of nanomaterials should be negative, and the pH value should raise [50].

Moreover, with CNTs dispersions, the changes in Zeta potential and pH can be easily noticed because the number of counter ions close to the CNT nanoparticles surface is increased due to the presence of SDBS, which forms the electrical double layer. With the increase in concentration from 50 ppm to 100 ppm, an increase in the number of ions getting attached to the particle surface is achieved [46], resulting from the removal of the macromolecules of SDBS. This could explain the superior stability of the nanofuels with a CNT concentration of 100 ppm, which exhibits a zeta potential of -104.5 mV and represents a value 54% higher than a CNT concentration of 50 ppm.

Additionally, the stability obtained with a CNT concentration of 100 ppm also might be explained by the Derjaguin, Verway, Landau, and Overbeek (DVLO) theory [51,52]. DLVO theory refers to the equilibrium between nanoparticle interactions and the double electric layer. In this instance, a CNT concentration of 100 ppm results in the predominance of the double electric layer due to the presence of SDBS, which creates an absorption layer that surrounds the CNTs and, allows for the formation of smaller nanoparticles that stay dispersed in the fluid for a longer duration. In contrast, with a CNT concentration of 50 ppm, interactions between the nanoparticles are predominant, mostly mediated by Van der Waals forces, since the SDBS molecules probably formed macromolecules, as previously stated and, as a result, the nanoparticles are larger and settle more quickly.

Preprints (www.preprints.org) | NOT PEER-REVIEWED | Posted: 18 October 2023 doi:10.20944/preprints202310.1042.v1

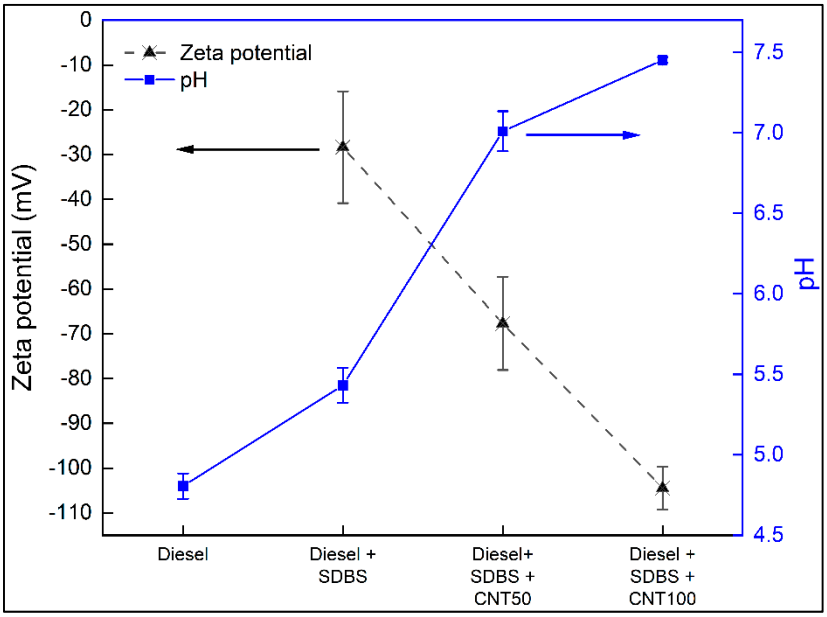

Figure 5. Zeta potential and pH measurements after nanofuels preparation at a CNT concentration of 100 ppm.

3.2. Thermal conductivity and surface tension of nanofuels

Figure 6 shows the measured thermal conductivities of diesel, diesel and SDBS, and nanofuels with CNTs at 20°C and 60°C after their preparation. A baseline using diesel was performed prior to the experimental design and compared to those suggested by the National Institute of Standards and Technology (NIST) [53]. In this case, standards for dodecane were taken into consideration, and a maximum error of 7% was found. According to the tests made at 20°C, the addition of SDBS to diesel resulted in a negligible increase in thermal conductivity, which would provide comparable outcomes during heat transfer processes. On the other hand, the dispersion of CNT at 50 ppm and 100 ppm exhibits thermal conductivity enhancements of approximately 2% and 4%, respectively. However, in terms of thermal conductivity, diesel and SDBS exhibit a negligible difference when compared to a CNT concentration of 50 ppm.

Nevertheless, the thermal conductivity of the base fluid decreases at 60 °C, and the findings can exhibit a closer relationship with what happens throughout the heating and evaporation processes. In this case, diesel thermal conductivity at 60°C is 12% lower than diesel at 20°C, as a result of the rise in thermal resistance with temperature. Besides, at 60 °C, thermal conductivity increased 4% with the SDBS addition to diesel. Although the inclusion of nanoparticles at a concentration of 50 ppm encouraged the decrease of thermal conductivity measurements, the large nanoparticle sizes and instability promoted measurement error. This is due to the many nanoparticles that are continuously subjected to Van der Waals forces and Brownian motion, which might have favored this negative effect [54], as was previously described. However, a CNT concentration of 100 ppm improved the thermal conductivity by about 20% compared to diesel at 60°C. This improvement may be attributed to the construction of thermal conductive grids for the avoidance of agglomeration due to SDBS presence because SDBS is attracted to the CNT surface, and the weakening of van der Waals forces at a suitable concentration [55]. Additionally, the stability provided for SDBS also inhibits large sedimentation rates, which improves the thermal conductivity by allowing Brownian motion [56] and reducing surface resistance at the nanoparticle-liquid and nanoparticle-nanoparticle interfaces [57].

Preprints (www.preprints.org) | NOT PEER-REVIEWED | Posted: 18 October 2023 doi:10.20944/preprints202310.1042.v1

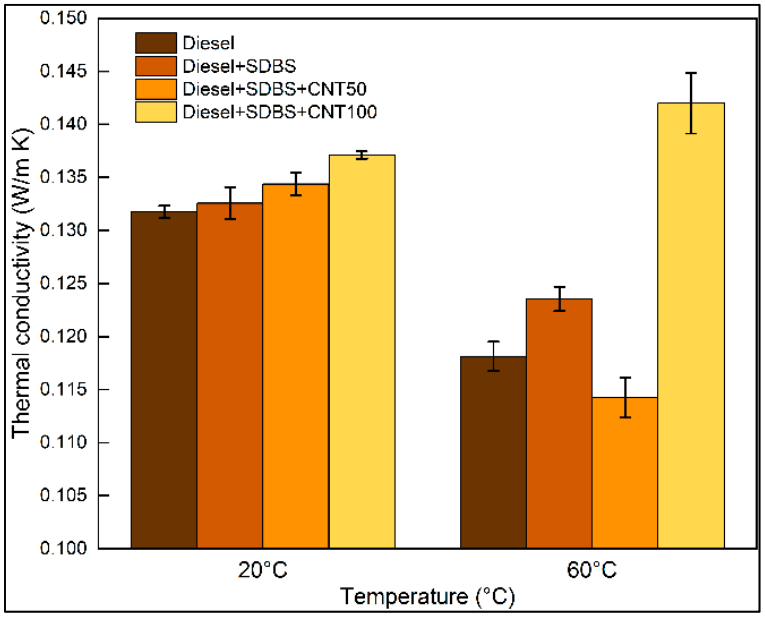

Figure 6. Thermal conductivity of nanofuels at 20°C and 60°C after preparation with CNTs at 50 ppm and 100 ppm stabilized with SDBS.

Figure 7 shows the surface tension obtained for diesel and the nanofuels with CNTS at 20°C and 60°C after their preparation. Since surface tension is a determinant factor because it can affect the atomization, spray tip penetration, evaporation, and combustion processes of the fuel [58]. Diesel and SDBS blends were also examined in order to analyze the effect of the addition of SDBS independently. Thus, adding SDBS to diesel lowers the surface tension because this surfactant is located at the liquid-air interface and produces a thin layer that lowers the surface energy [59]. However, Figure 7 shows results for diesel and SDBS blends that might be statistically comparable to those obtained with only diesel. This is because the concentration of surfactant used in this study is minimal enough to have an impact on surface tension, but it is enough to enhance the dispersion stability of CNTs in diesel, as was previously mentioned.

Additionally, as the temperature rose, surface tension decreased linearly because of weakening attractive interactions between diesel molecules. This is because they are subjected to a process of thermal expansion [60,61]. Findings show statistically that the surface tension has negligible changes in comparison to diesel and diesel - SDBS blends at a temperature of 20 °C when CNTs are added in concentrations of 50 ppm and 100 ppm. Likewise, the results reveal similar values between both concentrations at a temperature of 60 °C.

These findings are comparable to those of Mei, et al. [61], who demonstrate graphically that, when utilizing CTAB surfactant and CNT concentrations of 50 ppm and 100 ppm at 60°C, surface tension suffers a negligible increase of close to 2.5% and 4.6%, respectively. However, they point out that these minor changes result in an improvement in surface tension because this depends on the balance between the attractive force and the repulsive force, and the addition of nanoparticles implies that the attractive forces are significantly greater than the electrostatic repulsive force.

Nevertheless, the little variations depicted in Figure 7 indicate that the impact of surface tension is insignificant throughout the droplet combustion process since the utilization of SDBS and CNTs at the chosen concentrations is insignificant relative to the amount of diesel.

Preprints (www.preprints.org) | NOT PEER-REVIEWED | Posted: 18 October 2023 doi:10.20944/preprints202310.1042.v1

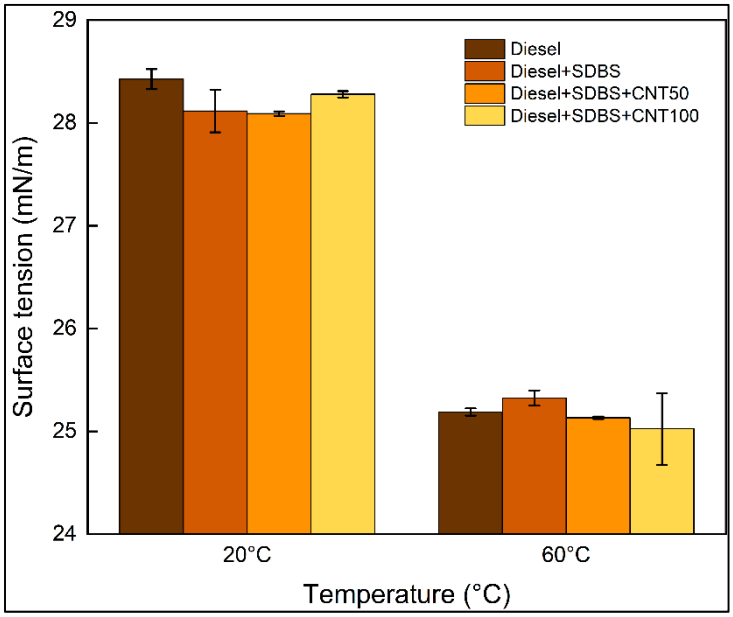

Figure 7. Surface tension of nanofuels at 20°C and 60°C after preparation with CNTs at 50 ppm and 100 ppm stabilized with SDBS.

3.3. Evolution of normalized area and ignition delay

Figure 8 shows the evolution of normalized area analysis of several samples employing diesel, SDBS, and CNTs at concentrations of 50 ppm and 100 ppm. The study was performed for 21 days to evaluate the impact of the nanofuels temporal stability. In this instance, tests were conducted utilizing four replicas of diesel, diesel - SDBS, and diesel - SDBS - CNTs. Additionally, at least ten drops of each fluid were burned and assessed in order to guarantee the accuracy of the findings. Thus, in Figure 8, each curve is surrounded by a shadow of a similar color to the center line, which represents the standard deviation between each replica.

It should be noted that the normalized area increases over one in the early parts of the lines as a consequence of the droplet expansion, which is a result of the volatile diesel components evaporation [26]. Then, there is a process where a maximum area peak is reached, and this is attributed to the ignition point, after which the sudden reduction in area is attached to the burning of the fuel. A detailed explanation of the characteristics of the curve is given in our previous work [43]. In the case of the area reduction of diesel and diesel - SDBS droplets, similar results were obtained, which is related to the negligible effect of the SDBS during combustion.

The burning time is predicted to decrease with the use of nanomaterials [28]. Nevertheless, combustion duration increased with the inclusion of CNTs at a concentration of 50 ppm (Figure 8a) in comparison to diesel and diesel - SDBS blends. In fact, the test on the preparation day (green line) indicates a prolonged combustion process and a hard start to the droplet burning. The findings of the normalized area after seven days reveal that there are negligible changes in combustion with regard to diesel and diesel - SDBS because the addition of CNTs at such concentrations could cause the ignition to take longer to start because of its slower burning rate. This is likely due to the CNTs tendency to be thermally resistant because of the high agglomeration rate caused by poor stability. That is, during combustion, the nanomaterials are positioned at the interface of the droplet, where they form a layer [24]. Thus, the thick multi-wall structure of the CNTs and the large agglomerates cause the temperature of the layer to rise more slowly during the heating and combustion processes, which prevents heat transfer to the fuel within the droplet [19]. As a result, the overall duration of the combustion process is expanded, which could result in a longer ignition delay, a consequence of the nanofuels stability at CNTs concentration of 50 ppm [46].

On the contrary, CNT concentration of 100 ppm has shown better results during the combustion process, as shown in Figure 8b, since it has been observed that the combustion process for diesel and

Preprints (www.preprints.org) | NOT PEER-REVIEWED | Posted: 18 October 2023 doi:10.20944/preprints202310.1042.v1

diesel - SDBS takes less time after each period of seven days after the preparation. In this situation, a porous layer is similarly anticipated to form on the droplet surface. However, the layer is anticipated to be thinner at this concentration as a result of the stability depicted in Figure 4 and Figure 5 above, which favors the rate of heat transfer towards the inner of the droplet. This is due to the fact that when the particle size is reduced, the porosity tends to be higher than that of big agglomerates [62,63], since the formation of the agglomerates might induce instability in the nanofuels and a decrease in porosity [64]. Therefore, at a CNT concentration of 100 ppm, the slower agglomeration of nanoparticles with time and the higher porosity relative to a concentration of 50 ppm provide enough time for the nanoparticles within the droplet to enhance the burning rate with sufficient nanoparticles acting as thermal bridges and multiple heterogeneous nucleation sites within the droplet [22].

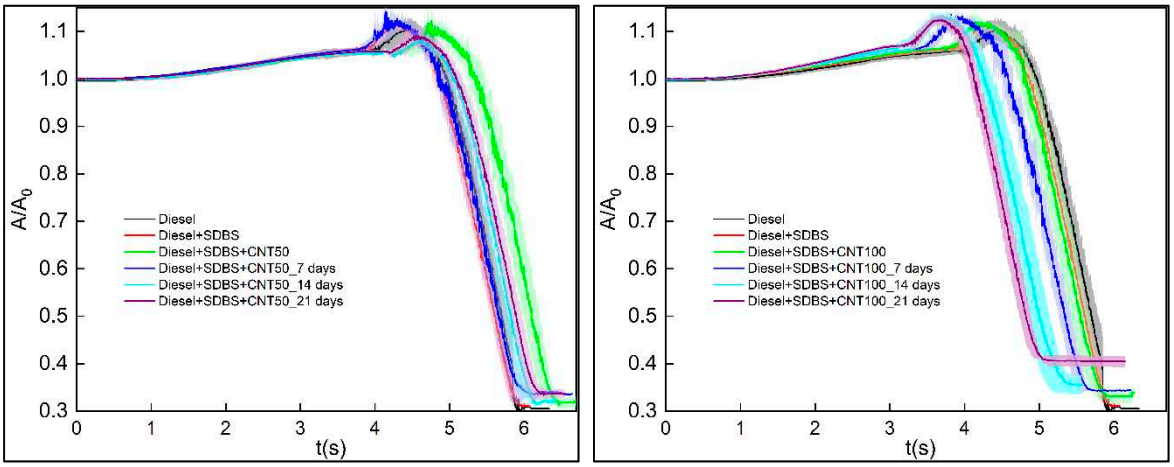

Figure 8. Evolution of normalized area of nanofuels during droplet combustion with diesel, SDBS and CNTs at concentrations of (a) 50 ppm and, (b) 100 ppm.

Otherwise, ignition delay refers to the amount of time required for the ignition to begin after the heating process has taken place (in this work, the activation of the electrical resistances). Physical and chemical delays are usually responsible for ignition delays. The physical delay is caused by the time required for the fuel to vaporize and the creation of combustible blends, whereas the chemical delay is caused by the hold-up in the fuel and air combustion reactions [65].

Figure 9 shows the ignition delay results after considering the temporal stability of the nanofuels. The ignition delay was determined at 95% of the time when the maximum peak expansion area occurred for each test. However, because droplet combustion is a very unexpected and difficult to replicate phenomenon, certain differences can be seen, such as those indicated by the standard deviation, because processes including heat transfer, thermal expansion, and evaporation are subject to rapid changes [66].

Thus, after preparation, the findings from using CNTs are comparable to those from using diesel and diesel - SDBS, although when a concentration of 50 ppm is tested, the ignition delay rises by around 7.6% in comparison to using diesel and diesel - SDBS. In fact, during the course of the 21-day test period, the ignition delay using nanofuels at a concentration of 50 ppm got worse. The limited stability of the nanofuels at such a concentration has an impact on the ignition time, indicating that this finding is closely connected to those in Figure 8a.

As was already explained, this outcome is linked to the formation of large agglomerates, which act as thermal resistances within the droplet and obstruct heat transfer. Additionally, the layer that forms at the interface encircles the droplet and absorbs additional heat, slowing the heating process. As a result, there is limited internal bubble nucleation, and the majority of burning only happens close to layer formation [22].

However, the use of CNTs at 100 ppm had the opposite effect, because improvements in ignition delay of about 3.5%, 11%, 16.2%, and 15.3% were observed with respect to diesel, at the day of preparation, and after 7, 14 and 21 days, respectively. In this approach, the high stability and

Preprints (www.preprints.org) | NOT PEER-REVIEWED | Posted: 18 October 2023 doi:10.20944/preprints202310.1042.v1

improvements in thermal conductivity demonstrated by the presence of these nanomaterials may be used to explain the improvement achieved by the addition of 100 ppm of CNTs to diesel. Furthermore, the characteristics mentioned by other research were reached with this concentration, such as high reactivity, fast burning, and a lower temperature required for ignition [26,66]. These factors together produced superior results with the use of CNTs at 100 ppm. Therefore, nanofuels may potentially be employed in practical applications and have superior properties than diesel throughout time, since improvements in ignition delay may directly impact the efficiency and emissions of harmful gases from diesel engines [67,68].

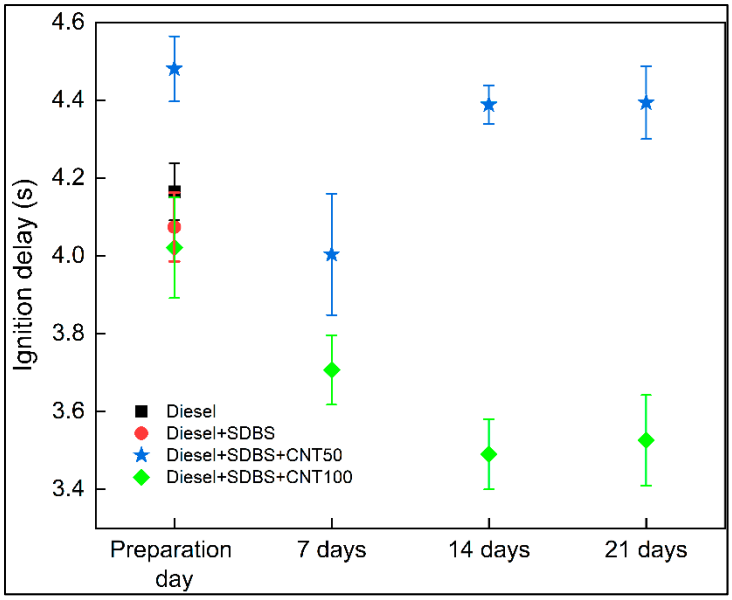

Figure 9. Temporal analysis of ignition delay of nanofuels during droplet combustion with diesel, SDBS and CNTs at concentrations of 50 ppm and 100 ppm.

3.4. Burning rate analysis

The rate of diffusion-controlled combustion between air and fuel in the vaporized state is referred to as the burning rate of a droplet. When examined in detail, as in the case of diesel engines, this parameter has a significant impact on performance and emission characteristics [65]. In this work, the burning rate constant of each droplet was assessed inside the burning zone of the droplet, using the D^2 law provided in Equation (1).

The transient burning rate curves of the tested nanofuels with respect to time are shown in Figure 10. The curves have a direct relationship with the ignition delay (Figure 9), and the area reduction curves (Figure 8). In fact, the findings are consistent across all analyses. For instance, negligible changes are found using SDBS in comparison to diesel. Likewise, the results obtained with the usage of CNTs at a concentration of 50 ppm are unpromising, as previously mentioned. This is a consequence of the increase in ignition delay up to 7% with respect to diesel. Therefore, the curves are shown starting at much longer time values than the diesel and diesel - SDBS curves. In fact, over the 21-day test period, the maximum burning rate was never larger than the maximum for diesel and diesel + SDBS. On the contrary, the results show that at concentrations of 50 ppm, the value of the combustion rate is reduced by up to 16%, which is consistent with the findings of the ignition delay (Figure 9) and is attributed to the decrease in stability that the nanofuels exhibit at such concentration, the limited increase in thermal conductivity, and the decrease in CNT porosity.

Figure 10 also shows the burning rate for the use of CNTs at a concentration of 100 ppm in comparison with diesel and diesel - SDBS. The findings are coherent with the area reduction curves (Figure 8) and the ignition delay results (Figure 9), since it is clear that using nanomaterials at this concentration enhances the burning rate over diesel and diesel - SDBS. The burning rate increases between 18% and 30.5%, which implies that the droplet lifetime is constantly lower. According to the

Preprints (www.preprints.org) | NOT PEER-REVIEWED | Posted: 18 October 2023 doi:10.20944/preprints202310.1042.v1

result, the highest burning rate (2.33 mm²/s) was reached after 7 days of preparation. Figure 9 demonstrates that while the nanofuels had a longer ignition delay at 7 days than at 14 days and 21 days, the burning rate upon ignition was substantially greater. That result is a consequence of the following features: First, the colloidal stability of the dispersion of CNTs with adsorbed molecules on their surface is guaranteed by the electrostatic repulsion given the presence of SDBS [69]. Second, this electrostatic repulsion restricts the agglomeration of the nanoparticles and, as a result, the porosity is maintained [62,63] and the active nucleation sites are preserved. Third, the concentration of 100 ppm has smaller particle sizes than the concentration of 50 ppm, which avoids the development of porous layers that prevent heat transfer toward the drop core and diffusion between the air and fuel [19]. Finally, research has demonstrated that the presence of nanomaterials can increase the thermal conductivity of the fuels (as shown in Figure 6), leading to higher combustion and evaporation rates [48]. However, since the best performance is demonstrated by a concentration of 100 ppm, after 21 days of preparation, the results must be evaluated broadly, since both the ignition delay and the burning rate impact the lifetime of the droplet.

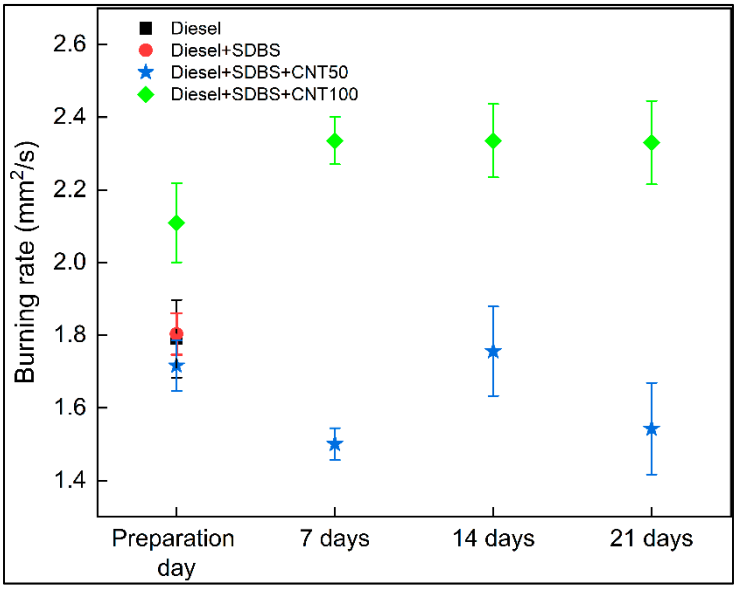

Figure 10. Effect of the CNTs and SDBS nanofuels temporal stability on the diesel droplet burning rate at CNTs concentrations of 50 ppm and 100 ppm.

As a special remark about the precedent results, the study of the ignition delay and burning that we performed in this work was done in a combustion chamber at atmospheric pressure, while combustion in compression ignition engines occurs at higher pressure. However, since some researchers have linked the properties of combustion or evaporation with the outcomes of applying nanofuels to diesel engines [32,70,71], the behavior in ignition delay and burning rate for a diesel engine may be comparable with the trends and implications of the present results. Those researchers claim that the increase in the rate of heat transfer and the high surface area/volume ratio that nanomaterials provide are likely the cause of the results found in this research, which may show the possibility of introducing nanomaterials in real engines.

3.5. Thermogravimetric analysis

Figure 11 shows the nanofuels thermogravimetric analysis (TGA), which included commercial diesel, SDBS, and CNTs blends at two concentrations, 50 ppm and 100 ppm. Figure 11 shows the evaporation process by heating at a rate of 10 °C/min in a nitrogen atmosphere between 25 and 250 °C. As a result, Figure 11a and c display the weight percentage decreasing in relation to the raise of the temperature. Test were carried out every week for 21 days after nanofuels preparation and at least three replicates were performed weekly. The same mass loss curve applies to all fuels. However,

Preprints (www.preprints.org) | NOT PEER-REVIEWED | Posted: 18 October 2023 doi:10.20944/preprints202310.1042.v1

this loss occurs at different temperatures because different factors may have an impact on the apparent heat of vaporization. As a consequence, the presence of SDBS and CNTs causes changes in physical properties (such as viscosity and nanofuels stability [72]) that affect the rate of vaporization.

In this case, adding SDBS accelerates the rate of evaporation, since the weight loss percentage occurs at lower temperatures than for diesel. This could be because of diesel and SDBS have different thermophysical properties [73], therefore, using SDBS, the evaporation process is faster than when only diesel is evaporated. For instance, small droplets, such as those typical of micro-explosions, may thus separate from the fluid and enhance weight loss because, first, the small and detached droplets evaporate more quickly and, second, this surface separation produces greater heat transfer area [74]. Nevertheless, when CNTs are added to the diesel-SDBS blend at a concentration of 50 ppm, the weight loss with respect to temperature demonstrates that the nanofuels requires a higher temperature for its evaporation, as shown by the derivative of weight with respect to temperature (Figure 11b). This result was expected because of the poor stability (Figure 4 and Figure 5) and the droplet combustion results (Figure 8) at such concentration. As was previously stated, this might be caused by the possibility of thick surface layers of nanomaterials at the fuel interface, which would produce an additional heat resistance that prevents the evaporation process.

Besides, contrary to the findings of area reduction and burning rate, a CNT concentration of 100 ppm cannot enhance the evaporation process of the nanofuels (Figure 11c and d). This is likely to be a consequence of the fact that properties like surface tension, density, viscosity, and evaporation temperature are determining factors in the decomposition process in an inert atmosphere [75]. Additionally, the improvement of the evaporation process requires the presence of an oxidizing environment [29,76], since carbonaceous nanomaterials require high levels of oxidation during combustion and evaporation processes [19].

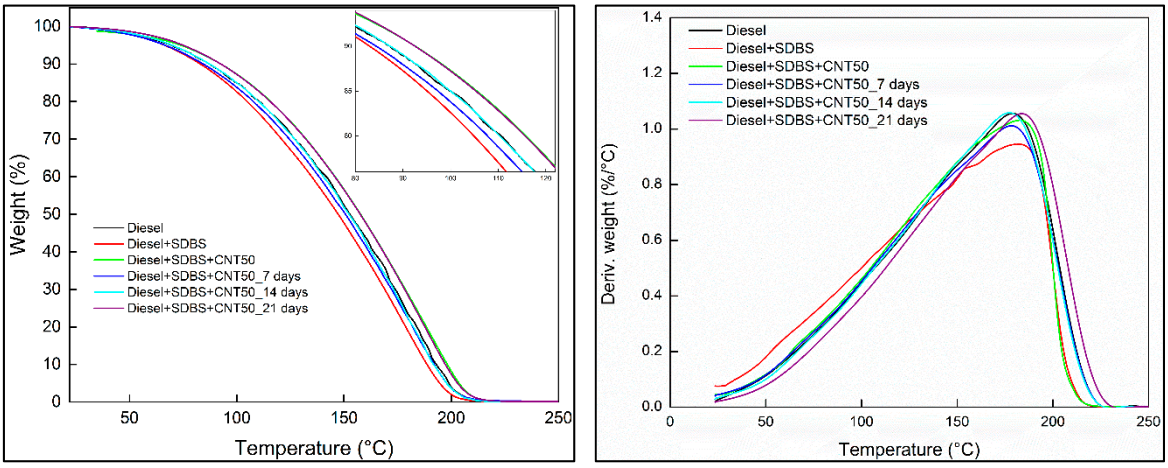

(a) (b)

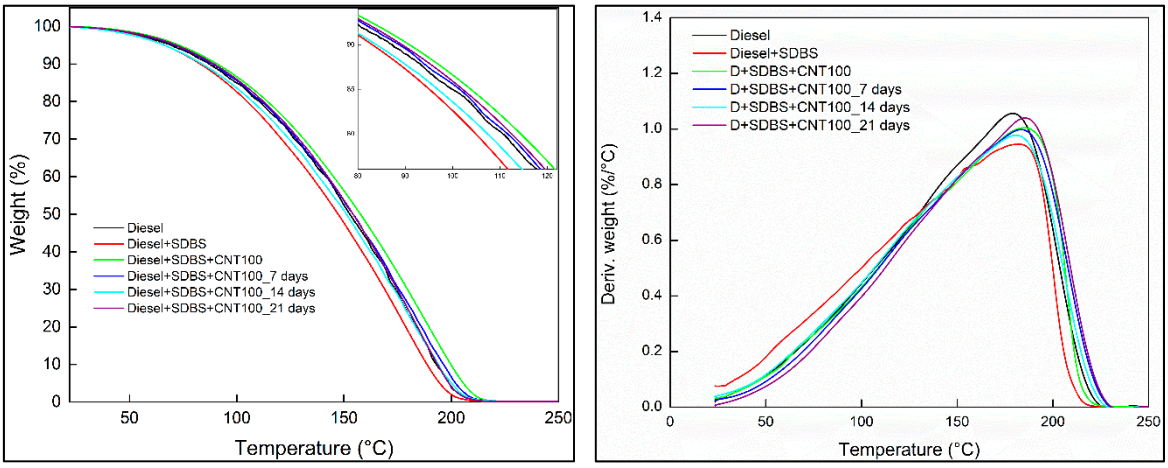

(c) (d)

 doi:10.20944/preprints202310.1042.v1

Figure 11. Temporal thermogravimetric analysis of diesel, SDBS and CNTs blends at concentrations of 50 ppm (a and b) and 100 ppm (c and d).

4. Conclusions

In this study, an experimental investigation of combustion parameters, such as ignition delay and burning rate, was conducted through the optical analysis of the combustion evolution of a single drop of commercial Colombian diesel containing a dispersion of pristine carbon nanotubes (CNT) and stabilized with sodium dodecyl benzene sulfonate (SDBS), using the shadowgraph technique. According to the results, the following conclusions were reached:

- Through the use of DLS, visual inspection, pH, and Zeta potential measurement, the nanofuels at a concentration of CNTs at 100 ppm were demonstrated to be more stable than those at 50 ppm. These findings might be explained by the presence of SDBS, which at a CNTs concentration of 50 ppm is probable to create macromolecules which promoted a decrease in stability. On the other hand, it is possible the existence of interactions between CNTs and SDBS at a concentration of 100 ppm because SDBS attaches to the surface of CNTs and forms an absorption layer that surrounds the nanomaterials and inhibits the formation of macromolecules, which significantly enhances temporal stability at this concentration.
- At 20 °C, the SDBS at a concentration of 0.02 w/v% in commercial diesel had a minimal impact on the thermal conductivity, while utilizing CNTs at a concentration of 50 ppm and 100 ppm, thermal conductivity increased 2% and 4%, respectively. However, at 60 °C, a concentration of 50 ppm showed negative effects on thermal conductivity, whereas with a concentration of 100 ppm, the thermal conductivity increased around 20%. On the other hand, the results indicate that when diesel -SDBS-CNT blends are used at temperatures between 20 °C and 60 °C, the surface tension has negligible changes in comparison to raw diesel.
- The duration of the combustion process is influenced by the stability of nanofuels at a concentration of 50 ppm, with greater durations for the first day and minimal changes after seven days for diesel and diesel - SDBS. However, concentration of 100 ppm provided better results, since the combustion of diesel and diesel-SDBS took less time after each interval of seven days. This is because, compared to a concentration of 50 ppm, nanoparticles aggregate more slowly and have higher porosity, giving them more time to improve combustion by acting as thermal bridges and having numerous heterogeneous nucleation sites within the droplet. Therefore, adding 50 ppm of CNTs to diesel causes the ignition delay time to increase by roughly 7.6%, and adding 100 ppm causes a decrease by roughly 16.2%.
- According to the data, the combustion rate is lowered by up to 16% at concentrations of 50 ppm. This is a result of the nanofuels decreased stability at this concentration, their limited increase in thermal conductivity, and their decreased porosity. On the contrary, at a concentration 100 ppm of CNT, the burning rate of diesel and diesel - SDBS was increased between 18% and 30.5%.

Author Contributions: **Anderson Gallego**: Methodology, Validation, Investigation, Formal analysis, Data curation, Writing – original draft. **Karen Cacua**: Conceptualization, Formal analysis. **Jorge Rentería**: Methodology, Software, Formal analysis, Data curation. **David Gamboa**: Validation, Formal analysis, Investigation, Data curation. **Bernardo Herrera**: Conceptualization, Methodology, Formal analysis, Writing – review & editing, Supervision, Project administration.

Acknowledgements: The authors wish to express their gratitude to Ministerio de Ciencia, Tecnología e Innovación de Colombia – Minciencias for the financing of the research program "Use of carbon nanomaterials as additives in diesel for internal combustion engines working in mode dual with natural gas and their effects on yield, pollutant emissions, and cell damage", as well as the work team of this program.

Conflicts of Interest: The authors declare no conflict of interest.

Nomenclature.

A/A0: Normalized area of the drop
CNT: Carbon nanotubes
DLS: Dynamic light scattering
K: Burning rate constant
SDBS: Sodium dodecylbenzene sulfonate
TGA: Thermogravimetric analysis

References

1. M. Shekofteh, T. M. Gundoshmian, A. Jahanbakhshi, and A. Heidari-Maleni, "Performance and emission characteristics of a diesel engine fueled with functionalized multi-wall carbon nanotubes (MWCNTs-OH) and diesel–biodiesel–bioethanol blends," *Energy Reports*, vol. 6, pp. 1438–1447, 2020, doi: 10.1016/j.egyr.2020.05.025.
2. J. Sadhik Basha, "Impact of Carbon Nanotubes and Di-Ethyl Ether as additives with biodiesel emulsion fuels in a diesel engine – An experimental investigation," *Journal of the Energy Institute*, vol. 91, no. 2, pp. 289–303, 2018, doi: 10.1016/j.joei.2016.11.006.
3. H. Griffiths, "Euro 7 standards: EU considers lifetime surveillance of every new car," Londres, Mar. 05, 2021. [Online]. Available: https://www.autoexpress.co.uk/news/354437/euro-7-standards-eu-considers-lifetime-surveillance-every-new-car
4. X. Guo, C. Liang, M. Umar, and N. Mirza, "The impact of fossil fuel divestments and energy transitions on mutual funds performance," *Technol Forecast Soc Change*, vol. 176, p. 121429, Mar. 2022, doi: 10.1016/j.techfore.2021.121429.
5. S. P. Jena, S. Mahapatra, and S. K. Acharya, "Optimization of performance and emission characteristics of a diesel engine fueled with Karanja biodiesel using Grey-Taguchi method," *Mater Today Proc*, vol. 41, pp. 180–185, 2021, doi: 10.1016/j.matpr.2020.08.579.
6. V. Saxena, N. Kumar, and V. K. Saxena, "Multi-objective optimization of modified nanofluid fuel blends at different TiO2 nanoparticle concentration in diesel engine: Experimental assessment and modeling," *Appl Energy*, vol. 248, no. December 2018, pp. 330–353, 2019, doi: 10.1016/j.apenergy.2019.04.091.
7. A. Yousefi, H. Guo, and M. Birouk, "Effect of diesel injection timing on the combustion of natural gas/diesel dual-fuel engine at low-high load and low-high speed conditions," *Fuel*, vol. 235, no. August 2018, pp. 838–846, 2019, doi: 10.1016/j.fuel.2018.08.064.
8. Q. Wu, X. Xie, Y. Wang, and T. Roskilly, "Effect of carbon coated aluminum nanoparticles as additive to biodiesel-diesel blends on performance and emission characteristics of diesel engine," *Appl Energy*, vol. 221, pp. 597–604, Jul. 2018, doi: 10.1016/j.apenergy.2018.03.157.
9. A. I. El-Seesy, A. M. A. Attia, and H. M. El-Batsh, "The effect of Aluminum oxide nanoparticles addition with Jojoba methyl ester-diesel fuel blend on a diesel engine performance, combustion and emission characteristics," *Fuel*, vol. 224, pp. 147–166, Jul. 2018, doi: 10.1016/j.fuel.2018.03.076.
10. H. Hosseinzadeh-Bandbafha *et al.*, "Effects of aqueous carbon nanoparticles as a novel nanoadditive in water-emulsified diesel/biodiesel blends on performance and emissions parameters of a diesel engine," *Energy Convers Manag*, vol. 196, pp. 1153–1166, Sep. 2019, doi: 10.1016/j.enconman.2019.06.077.
11. C. S. Aalam, C. G. Saravanan, and M. Kannan, "Experimental investigations on a CRDI system assisted diesel engine fuelled with aluminium oxide nanoparticles blended biodiesel," *Alexandria Engineering Journal*, vol. 54, no. 3, pp. 351–358, 2015, doi: 10.1016/j.aej.2015.04.009.
12. J. B. Ooi, H. M. Ismail, V. Swamy, X. Wang, A. K. Swain, and J. R. Rajanren, "Graphite Oxide Nanoparticle as a Diesel Fuel Additive for Cleaner Emissions and Lower Fuel Consumption," *Energy and Fuels*, vol. 30, no. 2, pp. 1341–1353, 2016, doi: 10.1021/acs.energyfuels.5b02162.
13. S. Kumar, P. Dinesha, and M. A. Rosen, "Effect of injection pressure on the combustion, performance and emission characteristics of a biodiesel engine with cerium oxide nanoparticle additive," *Energy*, vol. 185, pp. 1163–1173, 2019, doi: 10.1016/j.energy.2019.07.124.
14. S. Manigandan *et al.*, "Comparative study of nanoadditives TiO2, CNT, Al2O3, CuO and CeO2 on reduction of diesel engine emission operating on hydrogen fuel blends," *Fuel*, vol. 262, no. November 2019, 2020, doi: 10.1016/j.fuel.2019.116336.
15. T. Kegl, A. Kovač Kralj, M. Kegl, and B. Kegl, *Nanomaterials for Environmental Application*, vol. 10, no. July. in Green Energy and Technology, vol. 10. Cham: Springer International Publishing, 2020. doi: 10.1007/978-3-030-54708-0.
16. R. A. Alenezi, A. M. Norkhizan, R. Mamat, Erdiwansyah, G. Najafi, and M. Mazlan, "Investigating the contribution of carbon nanotubes and diesel-biodiesel blends to emission and combustion characteristics of diesel engine," *Fuel*, vol. 285, no. July 2020, p. 119046, 2021, doi: 10.1016/j.fuel.2020.119046.

17. Y. H. Bello *et al.*, "Investigating the engine performance, emissions and soot characteristics of CI engine fueled with diesel fuel loaded with graphene oxide-titanium dioxide nanocomposites," *Fuel*, vol. 269, p. 117436, Jun. 2020, doi: 10.1016/j.fuel.2020.117436.
18. S. Tanvir and L. Qiao, "Droplet burning rate enhancement of ethanol with the addition of graphite nanoparticles: Influence of radiation absorption," *Combust Flame*, vol. 166, pp. 34–44, Apr. 2016, doi: 10.1016/j.combustflame.2015.12.021.
19. S. Mosadegh, A. Ghaffarkhah, C. van der Kuur, M. Arjmand, and S. Kheirkhah, "Graphene oxide doped ethanol droplet combustion: Ignition delay and contribution of atomization to burning rate," pp. 1–45, 2021.
20. J. B. Ooi, H. M. Ismail, V. Swamy, X. Wang, A. K. Swain, and J. R. Rajanren, "Graphite Oxide Nanoparticle as a Diesel Fuel Additive for Cleaner Emissions and Lower Fuel Consumption," *Energy and Fuels*, vol. 30, no. 2, pp. 1341–1353, 2016, doi: 10.1021/acs.energyfuels.5b02162.
21. J. B. Ooi, J. R. Rajanren, H. M. Ismail, V. Swamy, and X. Wang, "Improving combustion characteristics of diesel and biodiesel droplets by graphite oxide addition for diesel engine applications," *Int J Energy Res*, vol. 41, no. 14, pp. 2258–2267, Nov. 2017, doi: 10.1002/er.3787.
22. A. F. Abdul Rasid and Y. Zhang, "Comparison of the burning of a single diesel droplet with volume and surface contamination of soot particles," *Proceedings of the Combustion Institute*, vol. 38, no. 2, pp. 3159–3166, Jan. 2021, doi: 10.1016/j.proci.2020.07.092.
23. G. Singh, M. Esmaeilpour, and A. Ratner, "Effect of carbon-based nanoparticles on the ignition, combustion and flame characteristics of crude oil droplets," *Energy*, vol. 197, Apr. 2020, doi: 10.1016/j.energy.2020.117227.
24. X. Wang *et al.*, "A comprehensive review on the properties of nanofluid fuel and its additive effects to compression ignition engines," *Appl Surf Sci*, vol. 504, no. January 2019, 2020, doi: 10.1016/j.apsusc.2019.144581.
25. T. Mesri Gundoshmian, A. Heidari-Maleni, and A. Jahanbakhshi, "Evaluation of performance and emission characteristics of a CI engine using functional multi-walled carbon nanotubes (MWCNTs-COOH) additives in biodiesel-diesel blends," *Fuel*, vol. 287, Mar. 2021, doi: 10.1016/j.fuel.2020.119525.
26. M. Dai, J. Wang, N. Wei, X. Wang, and C. Xu, "Experimental study on evaporation characteristics of diesel/cerium oxide nanofluid fuel droplets," *Fuel*, vol. 254, no. February, p. 115633, 2019, doi: 10.1016/j.fuel.2019.115633.
27. R. N. Mehta, U. More, N. Malek, M. Chakraborty, and P. A. Parikh, "Study of stability and thermodynamic properties of water-in-diesel nanoemulsion fuels with nano-Al additive," *Appl Nanosci*, vol. 5, no. 8, pp. 891–900, Nov. 2015, doi: 10.1007/s13204-014-0385-3.
28. X. Wang, N. Wei, J. Gao, J. Yan, and G. Jiang, "Evaporation Characteristics of Ethanol Diesel Droplets Containing Nanoparticles," *J Shanghai Jiaotong Univ Sci*, vol. 26, no. 2, pp. 201–209, Apr. 2021, doi: 10.1007/s12204-021-2280-x.
29. Muthukumar M, Senthil Kumar A P, Sasikumar C, Yuvaraj S, and T. S. Singh, "Effect of nanoparticles on the droplet combustion of rice bran oil biodiesel," *Biomass Convers Biorefin*, vol. 11, no. 4, pp. 1375–1393, Aug. 2021, doi: 10.1007/s13399-020-01209-8.
30. X. Wang, M. Dai, Y. Xie, J. Han, Y. Ma, and C. Chen, "Experimental investigation of evaporation characteristics of biodiesel-diesel blend droplets with carbon nanotubes and nanoceria as nanoadditives," *Appl Surf Sci*, vol. 505, no. January 2019, p. 144186, 2020, doi: 10.1016/j.apsusc.2019.144186.
31. K. Kannaiyan and R. Sadr, "The effects of alumina nanoparticles as fuel additives on the spray characteristics of gas-to-liquid jet fuels," *Exp Therm Fluid Sci*, vol. 87, pp. 93–103, Oct. 2017, doi: 10.1016/j.expthermflusci.2017.04.027.
32. R. Küçükosman, A. A. Yontar, and K. Ocakoglu, "Nanoparticle additive fuels: Atomization, combustion and fuel characteristics," *J Anal Appl Pyrolysis*, vol. 165, p. 105575, Aug. 2022, doi: 10.1016/j.jaap.2022.105575.
33. M. S. Gad and S. Jayaraj, "A comparative study on the effect of nano-additives on the performance and emissions of a diesel engine run on Jatropha biodiesel," *Fuel*, vol. 267, p. 117168, May 2020, doi: 10.1016/j.fuel.2020.117168.
34. S. N. A. Yusof, N. A. C. Sidik, Y. Asako, W. Mohd. A. A. Japar, S. B. Mohamed, and N. M. Muhammad, "A comprehensive review of the influences of nanoparticles as a fuel additive in an internal combustion engine (ICE)," *Nanotechnol Rev*, vol. 9, no. 1, pp. 1326–1349, Dec. 2020, doi: 10.1515/ntrev-2020-0104.
35. D. Liang *et al.*, "Effects of solids' concentration and oleic acid dispersant on the stability and combustion characteristics of aluminum/bioethanol nanofluid fuel," *Powder Technol*, vol. 398, p. 117108, Jan. 2022, doi: 10.1016/j.powtec.2022.117108.
36. K. Pandey, K. Chattopadhyay, and S. Basu, "Combustion dynamics of low vapour pressure nanofuel droplets," *Physics of Fluids*, vol. 29, no. 7, p. 074102, Jul. 2017, doi: 10.1063/1.4991752.
37. F. Dong, R. T. Koodali, H. Wang, and W. Ho, "Nanomaterials for Environmental Applications," *J Nanomater*, vol. 2014, pp. 1–4, 2014, doi: 10.1155/2014/276467.

38. V. Saxena, N. Kumar, and V. K. Saxena, "Multi-objective optimization of modified nanofluid fuel blends at different TiO2 nanoparticle concentration in diesel engine: Experimental assessment and modeling," *Appl Energy*, vol. 248, pp. 330–353, Aug. 2019, doi: 10.1016/j.apenergy.2019.04.091.
39. S. Sayyed, R. K. Das, and K. Kulkarni, "Experimental investigation for evaluating the performance and emission characteristics of DICI engine fueled with dual biodiesel-diesel blends of Jatropha, Karanja, Mahua, and Neem," *Energy*, vol. 238, p. 121787, Jan. 2022, doi: 10.1016/j.energy.2021.121787.
40. A. I. EL-Seesy, M. S. Waly, H. M. El-Batsh, and R. M. El-Zoheiry, "Enhancement of the waste cooking oil biodiesel usability in the diesel engine by using n-decanol, nitrogen-doped, and amino-functionalized multi-walled carbon nanotube," *Energy Convers Manag*, vol. 277, p. 116646, Feb. 2023, doi: 10.1016/j.enconman.2022.116646.
41. S. Mosadegh, A. Ghaffarkhah, C. van der Kuur, M. Arjmand, and S. Kheirkhah, "Graphene oxide doped ethanol droplet combustion: Ignition delay and contribution of atomization to burning rate," pp. 1–45, 2021, [Online]. Available: http://arxiv.org/abs/2104.13544
42. J. Wang *et al.*, "Flame spread and combustion characteristics of two adjacent jatropha oil droplets," *Fuel*, vol. 285, no. August 2020, p. 119077, 2021, doi: 10.1016/j.fuel.2020.119077.
43. J. Rentería, A. Gallego, D. Gamboa, K. Cacua, and B. Herrera, "Effect of amide-functionalized carbon nanotubes as commercial diesel and palm-oil biodiesel additives on the ignition delay: A study on droplet scale," *Fuel*, vol. 338, Apr. 2023, doi: 10.1016/j.fuel.2022.127202.
44. A. Braeuer, *In situ Spectroscopic Techniques at High Pressure*. in ISSN. Elsevier Science, 2015.
45. C. K. Law, "Recent advances in droplet vaporization and combustion," *Prog Energy Combust Sci*, vol. 8, no. 3, pp. 171–201, 1982, doi: 10.1016/0360-1285(82)90011-9.
46. S. Balamurugan and V. Sajith, "Experimental investigation on the stability and abrasive action of cerium oxide nanoparticles dispersed diesel," *Energy*, vol. 131, pp. 113–124, 2017, doi: 10.1016/j.energy.2017.05.032.
47. H. Dautzenberg, "Polymeric stabilization of colloidal dispersions.," *Acta Polymerica*, vol. 36, no. 8, pp. 457–457, Aug. 1985, doi: 10.1002/actp.1985.010360819.
48. R. Küçükosman, A. A. Yontar, and K. Ocakoglu, "Nanoparticle additive fuels: Atomization, combustion and fuel characteristics," *J Anal Appl Pyrolysis*, vol. 165, p. 105575, Aug. 2022, doi: 10.1016/j.jaap.2022.105575.
49. J. Liu *et al.*, "Applications of functional nanoparticle–stabilized surfactant foam in petroleum-contaminated soil remediation," *J Hazard Mater*, vol. 443, p. 130267, Feb. 2023, doi: 10.1016/j.jhazmat.2022.130267.
50. N. Ali, J. A. Teixeira, and A. Addali, "A Review on Nanofluids: Fabrication, Stability, and Thermophysical Properties," *Journal of Nanomaterials*, vol. 2018. Hindawi Limited, 2018. doi: 10.1155/2018/6978130.
51. G. Hwang *et al.*, "Analysis of stability behavior of carbon black nanoparticles in ecotoxicological media: Hydrophobic and steric effects," *Colloids Surf A Physicochem Eng Asp*, vol. 554, no. June, pp. 306–316, 2018, doi: 10.1016/j.colsurfa.2018.06.049.
52. Q. Lin, M. Xu, Z. Cui, X. Pei, J. Jiang, and B. Song, "Structure and stabilization mechanism of diesel oil-in-water emulsions stabilized solely by either positively or negatively charged nanoparticles," *Colloids Surf A Physicochem Eng Asp*, vol. 573, pp. 30–39, Jul. 2019, doi: 10.1016/j.colsurfa.2019.04.046.
53. M. L. Huber, A. Laesecke, and R. Perkins, "Transport Properties of n-Dodecane," *Energy & Fuels*, vol. 18, no. 4, pp. 968–975, Jul. 2004, doi: 10.1021/ef034109e.
54. A. Gallego, K. Cacua, B. Herrera, D. Cabaleiro, M. M. Piñeiro, and L. Lugo, "Experimental evaluation of the effect in the stability and thermophysical properties of water-Al2O3 based nanofluids using SDBS as dispersant agent," *Advanced Powder Technology*, vol. 31, no. 2, pp. 560–570, Feb. 2020, doi: 10.1016/j.apt.2019.11.012.
55. L. Liu, X. Zhang, and X. Lin, "Experimental investigations on the thermal performance and phase change hysteresis of low-temperature paraffin/MWCNTs/SDBS nanocomposite via dynamic DSC method," *Renew Energy*, vol. 187, pp. 572–585, Mar. 2022, doi: 10.1016/j.renene.2022.01.098.
56. M. E. M. Soudagar, N. N. Nik-Ghazali, M. Abul Kalam, I. A. Badruddin, N. R. Banapurmath, and N. Akram, "The effect of nano-additives in diesel-biodiesel fuel blends: A comprehensive review on stability, engine performance and emission characteristics," *Energy Convers Manag*, vol. 178, no. September, pp. 146–177, 2018, doi: 10.1016/j.enconman.2018.10.019.
57. E. v. Timofeeva *et al.*, "Thermal conductivity and particle agglomeration in alumina nanofluids: Experiment and theory," *Phys Rev E*, vol. 76, no. 6, p. 061203, Dec. 2007, doi: 10.1103/PhysRevE.76.061203.
58. B. Esteban, J. R. Riba, G. Baquero, R. Puig, and A. Rius, "Characterization of the surface tension of vegetable oils to be used as fuel in diesel engines," *Fuel*, vol. 102, pp. 231–238, Dec. 2012, doi: 10.1016/j.fuel.2012.07.042.
59. X. Wang, M. Dai, J. Wang, Y. Xie, G. Ren, and G. Jiang, "Effect of ceria concentration on the evaporation characteristics of diesel fuel droplets," *Fuel*, vol. 236, no. September 2018, pp. 1577–1585, 2019, doi: 10.1016/j.fuel.2018.09.085.
60. M. H. U. Bhuiyan, R. Saidur, R. M. Mostafizur, I. M. Mahbubul, and M. A. Amalina, "Experimental investigation on surface tension of metal oxide-water nanofluids," *International Communications in Heat and Mass Transfer*, vol. 65, pp. 82–88, Jul. 2015, doi: 10.1016/j.icheatmasstransfer.2015.01.002.

61. D. Mei, Y. Fang, Z. Zhang, D. Guo, Z. Chen, and C. Sun, "Analysis of surface tension for nano-fuels containing disparate types of suspended nanoparticles," *Powder Technol*, vol. 388, pp. 526–536, Aug. 2021, doi: 10.1016/j.powtec.2021.05.002.
62. M. Kubo, Y. Ishihara, Y. Mantani, and M. Shimada, "Evaluation of the factors that influence the fabrication of porous thin films by deposition of aerosol nanoparticles," *Chemical Engineering Journal*, vol. 232, pp. 221–227, 2013, doi: 10.1016/j.cej.2013.07.097.
63. J. Liu, J. J. Swanson, D. B. Kittelson, D. Y. H. Pui, and J. Wang, "Microstructural and loading characteristics of diesel aggregate cakes," *Powder Technol*, vol. 241, pp. 244–251, 2013, doi: 10.1016/j.powtec.2013.03.028.
64. L. Wang, K. J. Dong, C. C. Wang, R. P. Zou, Z. Y. Zhou, and A. B. Yu, "Computer simulation of the packing of nanoparticles," *Powder Technol*, vol. 401, pp. 1–10, 2022, doi: 10.1016/j.powtec.2022.117317.
65. M. R. Chow *et al.*, "Effects of ethanol on the evaporation and burning characteristics of palm-oil based biodiesel droplet," *Journal of the Energy Institute*, vol. 98, no. May, pp. 35–43, 2021, doi: 10.1016/j.joei.2021.05.008.
66. G. Jiang, J. Yan, G. Wang, M. Dai, C. Xu, and J. Wang, "Effect of nanoparticles concentration on the evaporation characteristics of biodiesel," *Appl Surf Sci*, vol. 492, no. June, pp. 150–156, 2019, doi: 10.1016/j.apsusc.2019.06.118.
67. S. Gumus, H. Ozcan, M. Ozbey, and B. Topaloglu, "Aluminum oxide and copper oxide nanodiesel fuel properties and usage in a compression ignition engine," *Fuel*, vol. 163, pp. 80–87, 2016, doi: 10.1016/j.fuel.2015.09.048.
68. A. K. Agarwal, J. G. Gupta, and A. Dhar, "Potential and challenges for large-scale application of biodiesel in automotive sector," *Prog Energy Combust Sci*, vol. 61, pp. 113–149, 2017, doi: 10.1016/j.pecs.2017.03.002.
69. R. Dubey, D. Dutta, A. Sarkar, and P. Chattopadhyay, "Functionalized carbon nanotubes: synthesis, properties and applications in water purification, drug delivery, and material and biomedical sciences," *Nanoscale Adv*, vol. 3, no. 20, pp. 5722–5744, 2021, doi: 10.1039/D1NA00293G.
70. J. Sadhik Basha and R. B. Anand, "The influence of nano additive blended biodiesel fuels on the working characteristics of a diesel engine," *Journal of the Brazilian Society of Mechanical Sciences and Engineering*, vol. 35, no. 3, pp. 257–264, Oct. 2013, doi: 10.1007/s40430-013-0023-0.
71. D. Mei, X. Li, Q. Wu, and P. Sun, "Role of Cerium Oxide Nanoparticles as Diesel Additives in Combustion Efficiency Improvements and Emission Reduction," *Journal of Energy Engineering*, vol. 142, no. 4, Dec. 2016, doi: 10.1061/(ASCE)EY.1943-7897.0000329.
72. S. Tanvir and L. Qiao, "Effect of addition of energetic nanoparticles on droplet-burning rate of liquid fuels," in *Journal of Propulsion and Power*, American Institute of Aeronautics and Astronautics Inc., Jan. 2015, pp. 408–415. doi: 10.2514/1.B35500.
73. Y. Gan, Y. S. Lim, and L. Qiao, "Combustion of nanofluid fuels with the addition of boron and iron particles at dilute and dense concentrations," *Combust Flame*, vol. 159, no. 4, pp. 1732–1740, Apr. 2012, doi: 10.1016/j.combustflame.2011.12.008.
74. Y. Gan and L. Qiao, "Combustion characteristics of fuel droplets with addition of nano and micron-sized aluminum particles," *Combust Flame*, vol. 158, no. 2, pp. 354–368, Feb. 2011, doi: 10.1016/j.combustflame.2010.09.005.
75. M. Nour, A. M. A. Attia, and S. A. Nada, "Improvement of CI engine combustion and performance running on ternary blends of higher alcohol (Pentanol and Octanol)/hydrous ethanol/diesel," *Fuel*, vol. 251, no. February, pp. 10–22, 2019, doi: 10.1016/j.fuel.2019.04.026.
76. H. Li, S. Pokhrel, M. Schowalter, A. Rosenauer, J. Kiefer, and L. Mädler, "The gas-phase formation of tin dioxide nanoparticles in single droplet combustion and flame spray pyrolysis," *Combust Flame*, vol. 215, pp. 389–400, 2020, doi: 10.1016/j.combustflame.2020.02.004.